

***In vivo* developmental biology study using noninvasive multi-harmonic generation microscopy**

Shi-Wei Chu, Szu-Yu Chen, Tsung-Han Tsai, and Tzu-Ming Liu

Department of Electrical Engineering and Graduate Institute of Electro-Optical Engineering, National Taiwan University, Taipei, 10617 Taiwan, R.O.C.

Cheng-Yung Lin and Huai-Jen Tsai

Institute of Molecular and Cell Biology, National Taiwan University, Taipei 10617, Taiwan, R.O.C.

Chi-Kuang Sun

Department of Electrical Engineering and Graduate Institute of Electro-Optical Engineering, National Taiwan University, Taipei, 10617 Taiwan, R.O.C.

Tel:+886-2-33665085. FAX:+886-2-23677467. Email: sun@cc.ee.ntu.edu.tw

Abstract: Morphological changes and complex developmental processes inside vertebrate embryos are difficult to observe noninvasively with millimeter-penetration and sub-micrometer-resolution at the same time. By using higher harmonic generation, including second and third harmonics, as the microscopic contrast mechanism, optical noninvasiveness can be achieved due to the virtual-level-transition characteristic. The intrinsic nonlinearity of harmonic generations provides optical sectioning capability while the selected 1230-nm near-infrared light source provides the deep-penetration ability. The complicated development within a ~1.5-mm thick zebrafish (*Danio rerio*) embryo from initial cell proliferation, gastrulation, to tissue formation can all be observed clearly *in vivo* without any treatment on the live specimen.

©2003 Optical Society of America

OCIS codes: 170.3880 Medical and biological imaging, 170.5810 Scanning microscopy, 170.6900 Three-dimensional microscopy, 190.1900 Diagnostic applications of nonlinear optics

References and links

1. G. Peleg, A. Lewis, M. Linial, and L. M. Loew, "Nonlinear optical measurement of membrane potential around single molecules at selected cellular sites," *Proc. Natl. Acad. Sci.* **96**, 6700-6704 (1999).
2. S.-W. Chu, I.-S. Chen, T.-M. Liu, C.-K. Sun, S.-P. Lee, B.-L. Lin, P.-C. Cheng, M.-X. Kuo, D.-J. Lin, and H.-L. Liu, "Nonlinear bio-photonics crystal effects revealed with multi-modal nonlinear microscopy," *J. Microscopy* **208**, 190-200 (2002).
3. P. J. Campagnola, A. C. Millard, M. Terasaki, P. E. Hoppe, C. J. Malone, and W. A. Mohler, "Three-dimensional high-resolution second-harmonic generation imaging of endogenous structural proteins in biological tissues," *Biophys. J.* **82**, 493-508 (2002).
4. M. Müller, J. Squier, K. R. Wilson, and G. J. Brakenhoff, "3D microscopy of transparent objects using third-harmonic generation," *J. Microsc.* **191**, 266-274 (1998).
5. D. Yelin and Y. Silberberg, "Laser scanning third-harmonic-generation microscopy in biology," *Opt. Express* **5**, 169-175 (1999), <http://www.opticsexpress.org/abstract.cfm?URI=OPEX-5-8-169>.
6. L. Canioni, S. Rivet, L. Sarger, R. Barille, P. Vacher, and P. Voisin, "Imaging of Ca²⁺ intracellular dynamics with a third-harmonic generation microscope," *Opt. Lett.* **26**, 515-517 (2001).
7. A. Y. Louie, M. M. Hüber, E. T. Ahrens, U. Rothbächer, R. Moats, R. E. Jacobs, S. E. Fraser, and T. J. Meade, "*In vivo* visualization of gene expression using magnetic resonance imaging," *Nat. Biotech.* **18**, 321-325 (2000).
8. F. S. Foster, C. J. Pavlin, K. A. Harasiewicz, D.A. Christopher, and D. H. Turnbull, "Advances in ultrasound biomicroscopy," *Ultrasound in Med. Biol.* **26**, 1-27 (2000).

9. S. A. Boppart, G. J. Tearney, B. E. Bouma, J. F. Southern, M. E. Brezinski, and J. G. Fujimoto, "Noninvasive assessment of the developing *Xenopus* cardiovascular system using optical coherence tomography," *Proc. Natl. Acad. Sci.* **94**, 4256-4261 (1997).
10. T. M. Yelbuz, M. A. Choma, L. Thrane, M. L. Kirby, and J. A. Izatt, "Optical coherence tomography: A new high-resolution imaging technology to study cardiac development in chick embryos," *Circulation* **106**, 2771-2774 (2002).
11. C. Palmes-Saloma and C. Saloma, "Long-depth imaging of specific gene expressions in whole-mount mouse embryos with single-photon excitation confocal fluorescence microscopy and FISH," *J. Struct. Bio.* **131**, 56-66 (2000).
12. J. M. Squirrell, D. L. Wokosin, J. G. White, and B. D. Bavister, "Long-term two-photon fluorescence imaging of mammalian embryos without compromising viability," *Nat. Biotech.* **17**, 763-767 (1999).
13. C. L. Phillips, L. J. Arend, A. J. Filson, D. J. Kojetin, J. L. Clendenon, S. Fang, and K. W. Dunn, "Three-dimensional imaging of embryonic mouse kidney by two-photon microscopy," *Am. J. Pathol.* **158**, 49-55 (2001).
14. R. R. Anderson and J. A. Parish, "The optics of human skin," *J. Invest. Dermat.* **77**, 13-19 (1981).
15. B. E. Bouma, G. J. Tearney, I. P. Bilinsky, B. Golubovic, and J. G. Fujimoto, "Self-phase-modulated Kerr-lens mode-locked Cr:forsterite laser source for optical coherence tomography," *Opt. Lett.* **21**, 1839 (1996).
16. S.-W. Chu, I-H. Chen, T.-M. Liu, P. C. Cheng, C.-K. Sun, and B.-L. Lin, "Multimodal nonlinear spectral microscopy based on a femtosecond Cr:forsterite laser," *Opt. Lett.* **26**, 1909-1911 (2001).
17. T.-M. Liu, S.-W. Chu, C.-K. Sun, B.-L. Lin, P. C. Cheng, and I. Johnson, "Multi-photon scanning microscopy using a femtosecond Cr:forsterite laser," *Scanning* **23**, 249-254 (2001).
18. A. Seas, V. Petričević, and R.R. Alfano, "Generation of sub-100-fs pulses from a CW mode-locked chromium-doped forsterite laser," *Opt. Lett.* **17**, 937-939 (1992).
19. C. B. Kimmel, W. W. Ballard, S. R. Kimmel, B. Ullmann, and T. F. Schilling, "Stages of embryonic development of the zebrafish," *Dev. Dynam.* **203**, 253-310 (1995).
20. J. M. Schins, T. Schrama, J. Squier, G. J. Brakenhoff, and M. Müller, "Determination of material properties by use of third-harmonic generation microscopy," *J. Opt. Soc. Am. B* **19**, 1627-1634 (2002).
21. K. König, P.T.C. So, W.W. Mantulin, and E. Gratton, "Cellular response to near-infrared femtosecond laser pulses in two-photon microscopes," *Opt. Lett.* **22**, 135-136 (1997).
22. A. Schönle and S. W. Hell, "Heating by absorption in the focus of an objective lens," *Opt. Lett.* **23**, 325-327 (1998).
23. I-H. Chen, S.-W. Chu, C.-K. Sun, P. C. Cheng, and B.-L. Lin, "Wavelength dependent damage in biological multi-photon confocal microscopy: a micro-spectroscopic comparison between femtosecond Ti:sapphire and Cr:forsterite laser sources," *Opt. Quantum. Electron* **34**, 1251-1266 (2002).
24. S.-W. Chu, T.-M. Liu, C.-K. Sun, C.-Y. Lin, and H.-J. Tsai, "Real-time second-harmonic-generation microscopy based on a 2-GHz repetition rate Ti:sapphire laser," *Optics Express* **11**, 933-938 (2003)
<http://www.opticsexpress.org/abstract.cfm?URI=OPEX-11-8-933>

1. Introduction

Highly penetrative and non-invasive *in vivo* light microscopy with <500-nm resolution has the potential of offering new insights into embryonic morphological and developmental studies. Optical higher harmonic-generation, including second harmonic generation (SHG) and third harmonic generation (THG), leaves no energy deposition to the interacted matters due to its virtual-level-transition characteristic, providing the optical "noninvasiveness" nature desirable for biological microscopy. The virtual-state-transition-based SHG and THG have been used to measure membrane potential [1], to locate bio-crystalline structure inside biological tissues [2], to image endogenous structural proteins [3], to observe cell morphology [4,5], and to detect Ca²⁺ intracellular dynamics [6]. Compared with other imaging techniques applicable to developmental biology such as magnetic resonance imaging [7], ultrasound imaging [8], optical coherence tomography [9, 10], confocal fluorescence microscopy [11], and two-photon fluorescence microscopy [12,13], the main advantage of our developed harmonics optical microscopy (HOM) is the combination of its sub-micrometer three-dimensional (3D) resolution, millimeter-penetration depth, and optical noninvasiveness. Due to the nonlinear nature, the generated SHG/THG intensities depend on the square/cubic of the incident light intensity. Similar to the multi-photon induced fluorescence process, this nonlinear dependency allows localized excitation and is ideal for intrinsic optical sectioning in laser scanning microscopy. By using endogenous harmonic-generations as the contrast mechanism, no fluorescence is required and the common issues of photodamage, phototoxicity, photobleaching, or dye availability can all be eliminated. It is thus important to fully utilize these endogenous harmonics signals for imaging purpose to replace unnecessary usage of

invasive and toxic fluorophores in common multi-photon fluorescence microscopy. This is especially important for *in vivo* studies of animal and human subjects since not all vertebrate tissues are autofluorescent, not to mention that the energy release in the fluorescence stimulating process would cause photodamages to the observed live specimens.

Since the generation of optical harmonics has a weak dependency on the excitation wavelength, we are thus allowed to choose the desirable light source that can provide high penetration through turbid specimens with minimized unwanted light-tissue interactions including scattering, absorption, and photodamage. Due to the combination of diminishing scattering cross section with longer wavelength and avoiding resonant molecular absorption of common tissue constituents such as water [14-16], light attenuation in a live biological specimen reaches a minimum around 1200~1350-nm wavelength. We choose the 1200~1350-nm excitation wavelength regime not only to provide high penetration and low photodamage but also to allow both SHG/THG to fall within the visible spectrum. Based on a Cr:forsterite femtosecond laser [15,17,18] centered at 1230-nm, falling in the transparency window of most biological specimens, here we demonstrate a noninvasive and highly penetrative higher-harmonics optical microscopy with a sub-micrometer spatial resolution. The detailed developmental processes within a ~1.5-mm thick zebrafish (*Danio rerio*) embryo from the initial cell proliferation, gastrulation, to tissue formation can all be observed clearly *in vivo* without any treatment on the live specimens. The excellent 3D resolution of the demonstrated HOM system (~0.4- μm lateral resolution, estimated from the full width half maximum of the THG signal across cellular membranes) allows us to capture the subtle developmental information on the cellular or sub-cellular levels deep inside the live embryos and larvae.

2. Harmonics optical microscope setup

Our home-built laser scanning HOM system is adapted from an Olympus FV300 scanning unit combined with an Olympus BX51 upright microscope while all optics are modified to allow the passage of the 1200~1350-nm infrared light. The collimated laser beam of a femtosecond Cr:forsterite laser is coupled into the scanning system connecting to the Olympus BX51 microscope with an aperture fitting tube lens. Real-time scanning is accomplished through the high-speed galvanometer mirrors inside the FV300. In order to visualize all cell activities inside a live zebrafish embryo, the working distance of the chosen objective has to be longer than the embryo thickness (>1.5-mm), including the chorion. The excitation laser pulse is focused into the desired location inside the specimen and scanning with a spot size close to its diffraction limit with a 2-mm-working-distance high numerical-aperture (NA) infrared objective (LUMPlanFI/IR 60X/water/NA 0.90, Olympus). The forward-propagated harmonics are collected using a high-NA (1.4) oil-immersion condenser. For multi-harmonics intensity mapping, two photomultiplier tubes (R928P, Hamamatsu), which are synchronized with the galvanometer mirrors, are used to respectively record the filtered SHG and THG intensities point by point to form two-dimensional sectioned images. To observe moving live specimens, the recording speed is chosen between 0.25-2.5 seconds per frame with 512X512-scanned points. Faster and slower acquisition rates would both result in the degradation of signal-to-noise ratio and image quality, either due to reduced signal intensity or specimen movement. The live and free-moving wild-type zebrafish fertilized eggs are kept inside an aquarium formed by slide glasses for observation. No treatment was applied to the live embryos. All the developmental stage nomenclatures are after Kimmel *et al.* [19].

3. Experimental results

The sectioning and the noninvasive characteristics of SHG/THG allow us to observe the 3D cell proliferation processes inside a zebrafish embryo *in vivo*. Due to the optical inhomogeneity in biological tissues, the signal contrast in the THG modality reflects the various interfaces inside a single cell [5,16,20] such as the spatial variations of linear or nonlinear susceptibility between nuclear membranes and cytoplasm or between cell membranes and their surrounding fluid. Moreover, since there is non-vanishing third order nonlinear susceptibility for all materials, the THG modality can be used as a general purpose

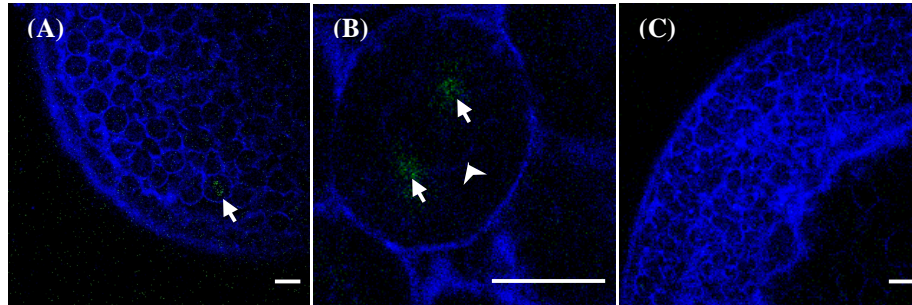


Fig. 1. Mitosis processes inside a live zebrafish embryo *in vivo* monitored with HOM. (a) An optical section of the embryo at the dome stage (4-hpf). The imaging depth is about 400- μm from the chorion surface. THG (shown in blue throughout this paper) picks up all interfaces including external yolk syncytial layers, cell membranes, and nuclear membranes while SHG (shown in green throughout this paper) shows the microtubule-formed spindle biconical array (indicated by the arrow). (b) (730-kB) Time series of the mitosis process in the embryonic blastoderm at 1-k cell stage (2.5-hpf). The cell nuclear membrane (arrowhead) and centrosomes (arrows) can be visualized through THG and SHG respectively. (c) (434 kB) Time series of the mitosis process in the embryonic blastoderm at shield-stage (6-hpf). Scale bar: 20- μm .

imaging tool. As a result, the cell structures in an embryo and the distribution of the organelles in a cell can be revealed by *in vivo* THG microscopy (Fig. 1). On the other hand, the contrast in SHG images corresponds to the distribution of crystalline nano-structures in biological samples where optical centro-symmetry is broken [3]. Centrosomes and mitotic spindles, for example, are made up of spatially organized dynamic microtubules. Therefore, strong SHG can be observed in the centrosomes and spindles as the blastoderm cells undergo mitosis (arrow in Fig. 1(a)). The dynamic changes of spindle and membrane between two daughter cells can be imaged *in vivo* by HOM without any exogenous markers (Fig. 1(a)). A circular cell nuclear membrane is clearly visualized through THG signals at the initial prophase stage while two centrosomes, revealed by SHG signals, are situated at the opposite sites of the nucleus. Strong SHG can be observed as the microtubules elongate from the centrioles to form the spindle at prometaphase. The alignment of chromosomes in the center of the cell during metaphase is disclosed by the broadening and flattening of the spindle (see the green part of the animation in Fig. 1(b)). The separation of spindle fibers and the alternation of the cell contour during anaphase are picked up by SHG and THG modalities, respectively. Endogenous SHG signal vanishes at telophase as the spindle microtubules disperse into the cells and exhibit no more crystalline characteristic. The cytokinesis process of the subsequent daughter cell membrane formation is monitored through the *in vivo* THG microscopy. A larger view of the *in vivo* THG microscopy showing the mitosis process at shield stage (6-hours post fertilization, 6-hpf) is given in Fig. 1(c), where the proliferated cells are migrating from the dorsal axis toward the edge of the blastoderm. No optical damage can be observed and the cell viability is preserved during the whole proliferation process even with a 100-mW incident average power on the embryo after 12-hour successive observations. The total energy injected into one embryo during the observation is more than 1-kJ (flux density $\approx 1.5 \times 10^7$ -W/cm²; 10- μs pixel dwell time). Compared with common multi-photon fluorescence technique using a 730~800-nm Ti:sapphire femtosecond laser at a similar experimental condition [21], Chinese hamster ovary cells were found to be unable to form clones with more than 6-mW average power and complete cell destruction occurs at an average power more than 10-mW. Even though increasing the excitation laser wavelength to 1047-nm will allow long-term two-photon fluorescence imaging of mammalian embryos without compromising viability, however the average illumination power was still limited to 13-mW while a total exposure of only 2-J could be applied to one embryo within a 24-hours imaging period [12]. Although there seems to exhibit a greater potential for sample heating at our NIR excitation wavelength due to water absorption, our experiments have proved that for a laser scanning system imaging optically transparent embryos, the potential heating due to water absorption is

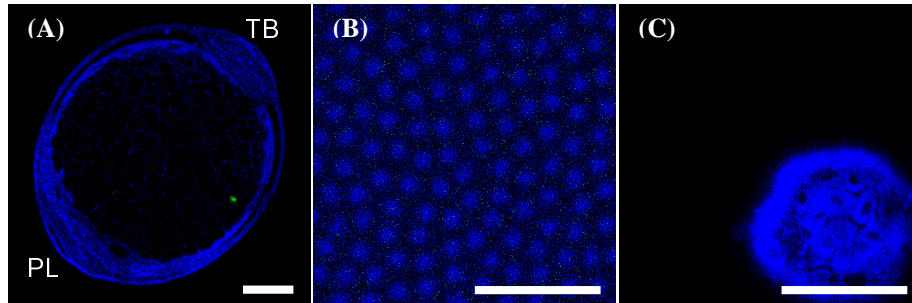


Fig. 2: *In vivo* HOM sectioning inside a live zebrafish embryo at the 2-somite stage. (a) A sectioning showing the whole embryo at a depth of 700- μm from the chorion surface (ventral view). PL: polster; TB: tail bud. (b) THG image of the chorion surface, showing the $<1\text{-}\mu\text{m}$ diameter granular canals and demonstrating the sub- μm resolution. (c) (738 kB) Depth-resolved optical section series at depths from 300- μm to 1400- μm inside the embryo. Scale bar: 100- μm except for B: 10- μm .

not a factor limiting viability with an illuminating wavelength as long as 1230 nm. According to the formula in Ref. [22], we have estimated the temperature change due to water absorption under 1230-nm excitation with 100-mW average power and a sample heating much less than 0.1- $^{\circ}\text{C}$ is obtained. Our successful long-term observation without compromising cell viability using 100-mW average power indicates not only negligible linear absorption with the infrared light at 1230-nm, but also the reduction of multi-photon damages [23]. We can successively monitor the development of the embryos throughout a continuous 12-hour period of time repeatedly and the examined embryos can all develop normally to larval stage after they are kept in the container for 1 day.

The excellent depth-resolution and high penetration capability of the HOM system are demonstrated in Fig. 2. Fig. 2(a) shows an *in vivo* optical section in the live zebrafish embryo at a depth of 700- μm from the chorion, showing the developing polster and tail bud (chorion is outside the viewing area of Fig. 2(a)). The yolk granule membranes and the semicrystalline membrane proteins in the yolk cells can be picked up by THG and SHG signals respectively. Moving the focus to the sample surface, THG signals reveal the 0.5-0.7- μm width granular canals distributed on the chorion surface (Fig. 2(b)), demonstrating its sub-micrometer resolution. At a depth of 350- μm from the chorion, the blastomere at the embryonic shield can be observed. Individual cell nucleus, cellular membranes, and the boundary of the blastomere can all be observed through the high-resolution THG modality due to their optical susceptibility differences with the surrounding media (Fig. 2(c)). Moving deeper into the blastoderm, the deep cell layers, the yolk cells, and the internal yolk syncytial layers all show up in the depth-resolved optical section series, confirming the capability of the THG microscopy to be a general non-invasive imaging tool for cell and tissue morphology. After viewing the densely packed yolk granules throughout the whole yolk with depth-resolved THG microscopy, the bottom of the yolk sphere can be observed at a depth of 1.26-mm from the top chorion surface while the lower side of chorion also shows up at the end of Fig. 2(c) (1.4-mm depth from the top surface). For imaging in specimens not as transparent as zebrafish embryos, the imaging depth and quality may be reduced due to the strong aberration of the illuminating light and absorption/scattering of the generated harmonics. Note that the images of yolk granules remain sharp all the way through the yolk and the sub-micrometer canals on the chorion are well-resolved even at the lower side, demonstrating the high penetration ability and indicating no serious aberration is induced as the long-wavelength infrared light penetrating $>1\text{-mm}$ through the embryo.

Besides observing the embryo developments, HOM is also applied to the examination of general tissue structures in live free-swimming larvae (Fig. 3). The general morphological structures, including the larva skin and the boundary of somite and notochord (Fig. 3(a)), can

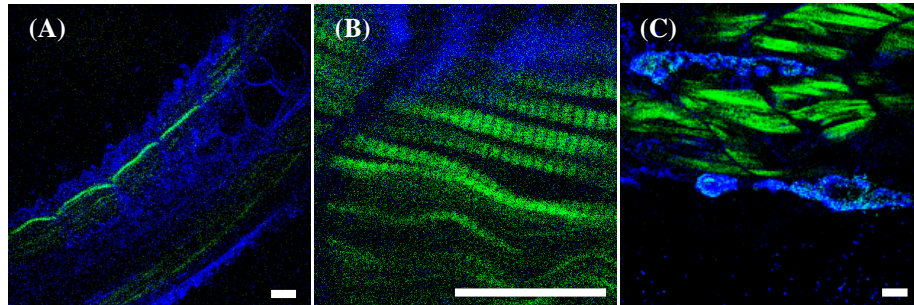


Fig. 3: *In vivo* HOM sectioning inside a live zebrafish larva at the 20-somite stage. (a) An optical section at the center of the larva showing the segments inside the vacuolated notochord and the distribution of somites alongside the notochord. (b) The enlarged view inside a somite showing individual muscle fiber and the sarcomeres on it through SHG as well as the interface between somites through THG. (c) (281 kB) Depth resolved optical series showing that we can visualize through a whole zebrafish larva with HOM. Scale bar: 20- μ m.

be revealed by THG signals. On the other hand, muscle fibers, which are composed of collaterally organized myosin and actin filaments, exhibit strong SHG emission due to its crystalline nano-structure [2,24]. The detailed distribution of muscle fibers in a somite can be observed (Fig. 3(b)) where individual sarcomere composed of A- and I-bands with a periodicity less than 2- μ m inside muscle fibers can be readily resolved, demonstrating again the superb spatial resolution provided by this powerful new technique. Again this highly penetrative HOM allows us to image through a live free-swimming zebrafish larva while all sub-micrometer-scaled morphological developments can be revealed. From the depth resolved optical section series in Fig. 3(c), the right side somites, the dorsal fin, and the left side somites of the larva are successively observed as we move the focus into the swimming reclined zebrafish, showing that the high penetration ability is still retained for larva imaging. Since dorsal fin is composed of collagen fibers, which are made up of parallelly packed nano-fibrils, strong SHG emission can also be observed.

4. Summary

To our knowledge, no other technique can provide such high-resolution, high-contrast *in vivo* images of the developmental processes deep inside live vertebrate embryos and larvae without extra labeling or handling. Due to the virtual-level-transition property of optical harmonic generations, truly noninvasive optical microscopy can be realized through the use of second and third harmonic generations as the contrast mechanism. No optical damage is induced and the cell viability is remained even after 12-hours successive observation with a 100-mW average power and >1-kJ energy injected into one fertilized egg. The intrinsic nonlinearity of higher harmonic generation provides the optical sectioning capability while the selected 1230-nm near-infrared light source provides the deep-penetration ability. The detailed developments within a ~1.5-mm thick zebrafish (*Danio rerio*) embryo from initial cell proliferation, gastrulation, to tissue formation can all be observed clearly *in vivo* without any treatment on the live specimens. This demonstrated multi-harmonic generation microscopy, a truly noninvasive microscopy, should be most suitable to the study of the 3D cytoarchitecture dynamics during embryogenesis with a sub-micrometer resolution and a millimeter penetration depth. This approach is also useful for studying cell-fate determination at early developmental stage.

Acknowledgments

This project is sponsored by National Health Research Institute (NHRI-EX92-9201EI), National Science Council (NSC-91-2215-E-002-021), and NTU Center for Genomic Medicine of Taiwan, R.O.C. S.-W. Chu would like to acknowledge the generous support from

MediaTek Incorporation, The correspondence should be addressed to C. K. Sun:
sun@cc.ee.ntu.edu.tw.